Integrated Transmission-Distribution Multi-Period Switching for Wildfire Risk Mitigation: Improving Speed and Scalability with Distributed Optimization

Preprint

Rachel Harris,[1] Chin-Yao Chang,[2] and Daniel K. Molzahn[1]

1 Georgia Institute of Technology
2 National Laboratory of the Rockies

Presented at the 16th IEEE PowerTech 2025
Kiel, Germany
June 29–July 3, 2025

The National Laboratory of the Rockies is a national laboratory of the U.S. Department of Energy, Office of Critical Minerals and Energy Innovation, operated under Contract No. DE-AC36-08GO28308.

This report is available at no cost from the National Laboratory of the Rockies (NLR) at www.nrel.gov/publications.

Conference Paper
NLR/CP-5D00-93128
January 2026

NATIONAL LABORATORY OF THE ROCKIES

Integrated Transmission-Distribution Multi-Period Switching for Wildfire Risk Mitigation: Improving Speed and Scalability with Distributed Optimization

Preprint

Rachel Harris,[1] Chin-Yao Chang,[2] and Daniel K. Molzahn[1]

1 Georgia Institute of Technology
2 National Laboratory of the Rockies

Suggested Citation
Harris, Rachel, Chin-Yao Chang, and Daniel K. Molzahn. 2026. *Integrated Transmission-Distribution Multi-Period Switching for Wildfire Risk Mitigation: Improving Speed and Scalability with Distributed Optimization: Preprint*. Golden, CO: National Laboratory of the Rockies. NLR/CP-5D00-93128. https://www.nrel.gov/docs/fy26osti/93128.pdf.

The National Laboratory of the Rockies is a national laboratory of the U.S. Department of Energy, Office of Critical Minerals and Energy Innovation, operated under Contract No. DE-AC36-08GO28308.

This report is available at no cost from the National Laboratory of the Rockies (NLR) at www.nrel.gov/publications.

Conference Paper
NLR/CP-5D00-93128
January 2026

National Laboratory of the Rockies
15013 Denver West Parkway
Golden, CO 80401
303-275-3000 • www.nrel.gov

NOTICE

This work was authored by the National Laboratory of the Rockies for the U.S. Department of Energy (DOE), operated under Contract No. DE-AC36-08GO28308. Funding provided by DOE Office of Electricity, Advanced Grid Modeling Program, through agreement NO. 33652. The views expressed herein do not necessarily represent the views of the DOE or the U.S. Government. The U.S. Government retains and the publisher, by accepting the article for publication, acknowledges that the U.S. Government retains a nonexclusive, paid-up, irrevocable, worldwide license to publish or reproduce the published form of this work, or allow others to do so, for U.S. Government purposes.

Cover photos (clockwise from left): Josh Bauer, National Laboratory of the Rockies 61725; Visualization from National Laboratory of the Rockies Insight Center; Getty-181828180; Agata Bogucka, National Laboratory of the Rockies 91683; Dennis Schroeder, National Laboratory of the Rockies 51331; Werner Slocum, National Laboratory of the Rockies 67842.

Integrated Transmission-Distribution Multi-Period Switching for Wildfire Risk Mitigation: Improving Speed and Scalability with Distributed Optimization

Rachel Harris
Georgia Institute of Technology
Atlanta, GA, USA
rharris94@gatech.edu

Chin-Yao Chang
National Renewable Energy Laboratory
Golden, CO, USA
chinyao.chang@nrel.gov

Daniel K. Molzahn
Georgia Institute of Technology
Atlanta, GA, USA
molzahn@gatech.edu

***Abstract*—With increasingly severe wildfire conditions driven by climate change, utilities must manage the risk of wildfire ignitions from electric power lines. During "public safety power shutoff" events, utilities de-energize power lines to reduce wildfire ignition risk, which may result in load shedding. Distributed energy resources provide flexibility that can help support the system to reduce load shedding when lines are de-energized. We investigate a coordinated transmission-distribution optimization problem that balances wildfire risk mitigation and load shedding. We model distribution systems that include battery energy storage systems which may support loads when transmission lines are de-energized. This multi-period integrated transmission-distribution optimal switching problem jointly optimizes line switching, generator setpoints, load shedding, and battery states of charge, posing significant computational challenges. To improve scalability, we decompose the problem over both space and time and apply a distributed optimization algorithm. Using a large-scale synthetic California test case with realistic distribution models and real wildfire risk data, we show that distributed optimization can solve large-scale multi-period switching problems that are otherwise intractable for centralized solvers. We also discuss challenges and future directions for improving the distributed algorithm's convergence performance as the number of time periods increases.**

***Index Terms*—Integrated transmission-distribution, distributed optimization, wildfire mitigation, mixed-integer linear program**

I. Introduction

Wildfires are expected to become more frequent and severe as the climate changes. To reduce wildfire ignition risk from electric power line faults, utilities may de-energize power lines during high-risk periods, a practice known as "public safety power shutoffs" [1]. De-energizing lines may cause power outages, motivating solutions that balance wildfire risk reduction while minimizing power outages.

This work was authored in part by NREL, operated by Alliance for Sustainable Energy, LLC, for the U.S. Department of Energy (DOE) under Contract No. DE-AC36-08GO28308. Funding provided by DOE Office of Electricity, Advanced Grid Modeling Program, through agreement NO. 33652. The views expressed in the article do not necessarily represent the views of the DOE or the U.S. Government. The U.S. Government retains and the publisher, by accepting the article for publication, acknowledges that the U.S. Government retains a nonexclusive, paid-up, irrevocable, worldwide license to publish or reproduce the published form of this work or allow others to do so, for the U.S. Government purposes.

This work was supported by the NSF AI Institute for Advances in Optimization (AI4OPT), #211253.

Prior work has explored optimal transmission switching for wildfire risk reduction [2], and incorporating equity to make power shutoffs more fair over time [3]. Recent work performed distribution network reconfiguration and microgrid formation to reduce wildfire risk [4], [5], and introduced formulations which are robust to uncerainty [6].

To the best of our knowledge, this paper formulates the first integrated transmission-distribution (ITD) co-optimization for wildfire risk mitigation. Distributed energy resources (DERs) provide flexibility to reduce outages during transmission switching. We jointly optimize transmission line de-energizations and distribution network operation over multiple time periods. The problem is a large-scale, multi-time-period mixed-integer linear program (MILP), which requires prohibitive amounts of time and memory to solve. To improve scalability, we decompose the problem over both space and time and apply the alternating direction method of multipliers (ADMM) distributed optimization algorithm to solve the decomposed problem.

Previous distributed approaches to ITD optimization used ADMM for multi-period economic dispatch [7], [8] and transmission-distribution reserve scheduling [9]. Prior work used small, balanced distribution networks. In contrast, we use realistic unbalanced synthetic distribution networks with thousands of buses each; our full test case contains over 10,000 buses. Although ADMM is not guaranteed to converge for non-convex problems, it may be used as a heuristic to solve mixed-integer programming problems [10]–[12]. ADMM may provide significant computational advantages compared to global solution methods like branch-and-bound, which suffer from exponential worst-case time complexity. We find that ADMM may solve the large optimal switching MILP much more quickly than a state-of-the-art centralized solver. However, when the number of time periods in our multi-period problem is sufficiently large, ADMM suffers from slow convergence or reaches consensus at a sub-optimal solution. We provide associated discussion in Section IV.

Our contributions are as follows:

1) We formulate and solve a transmission-distribution co-optimization problem to select transmission line de-energizations which minimize wildfire risk and load

shedding. This is the first work to coordinate transmission and distribution networks to optimize power shut-offs under wildfire risk.

2) We develop a scalable solution by decomposing over space and time and applying an ADMM-based distributed algorithm. To the best of our knowledge, this paper is the first to use ADMM to solve optimal switching problems for wildfire risk mitigation.
3) We present numerical results from large-scale, realistic systems. With a formulation that requires the transmission network to remain fully connected, our proposed distributed approach solves this optimal switching problem much more quickly than a centralized solver when considering up to eight time periods. We also show that coordinated transmission-distribution optimization produces switching decisions that reduce wildfire ignition risk compared to solving a transmission-level switching problem alone. Removing connectivity constraints to allow transmission islanding further reduces wildfire risk but increases computation time.

We organize the remainder of the paper as follows: Section II formulates the optimal switching problem, Section III details the distributed solution method, Section IV presents numerical results showing the improved performance from transmission-distribution coordination and computational advantages of the distributed approach, and Section V concludes.

II. Problem Formulation

We formulate the optimal switching problem to minimize a weighted sum of wildfire ignition risk and load shedding over multiple time periods. The constraints include standard power flow physics and engineering limits, augmented to support component shut-offs. The control variables are transmission line energization statuses, transmission generator setpoints, distribution bus load shed, and distribution storage system charge/discharge setpoints. A full nonlinear AC formulation with binary energization status variables yields a computationally intractable mixed-integer nonlinear program. The linearized LinDistFlow power flow approximation [13] is widely used to model power flow in distribution systems and, while less common, can also be used to approximate transmission system power flow models as well.

We use superscripts $\mathcal{H}$ and $\mathcal{D}$ to denote transmission and distribution components, respectively. Time periods are indexed by $t \in \mathcal{T} = \{1, 2, ..., T\}$. Power flow in the transmission network is modeled with a balanced single-phase LinDistFlow approximation, while we use an unbalanced three-phase LinDistFlow model for the distribution network. Following [14], we include constraints that balance the power flow and match voltage magnitudes at the transmission-distribution boundary.

A. Transmission Constraints

Consider a transmission network with a set of buses $\mathcal{N}^{\mathcal{H}}$ and a set of lines $\mathcal{L}^{\mathcal{H}}$. The active and reactive power flows through line (i,k) at time t are $p_{ik,t}$ and $q_{ik,t}$, respectively. The binary variables $\ell_{ik,t}$ represent the energization status at time $t \in \mathcal{T}$ of the transmission line $(i,k) \in \mathcal{L}^{\mathcal{H}}$ connecting bus i to bus k. Operational limits restrict the amount of power flow across lines. The lower bounds on active and reactive power flows are $\underline{p}_{ik}$ and $\underline{q}_{ik}$, while the upper bounds on active and reactive power flows are $\overline{p}_{ik}$ and $\overline{q}_{ik}$, respectively. The line flow is then defined as

$$\begin{aligned} \underline{p}_{ik}\ell_{ik,t} \le p_{ik,t} \le \overline{p}_{ik}\ell_{ik,t} \quad \forall (i,k) \in \mathcal{L}^{\mathcal{H}},\ \forall t \in \mathcal{T} \\ \underline{q}_{ik}\ell_{ik,t} \le q_{ik,t} \le \overline{q}_{ik}\ell_{ik,t} \quad \forall (i,k) \in \mathcal{L}^{\mathcal{H}},\ \forall t \in \mathcal{T} \end{aligned} \tag{1}$$

so that the active and reactive power flows $p_{ik,t}$ and $q_{ik,t}$ must be within their operational limits if line (i,k) is energized, and must be 0 if line (i,k) is de-energized.

Next, we introduce the notation $w_{i,t}$ to represent the squared voltage magnitude at bus i at time t. Also note that the line resistance is r_{ik} and the line reactance is x_{ik}. For all $(i,k) \in \mathcal{L}^{\mathcal{H}}$ and $t \in \mathcal{T}$, the voltage drop across line (i,k) is given as

$$\begin{aligned} 2(r_{ik}p_{ik,t} + x_{ik}q_{ik,t}) + (1-\ell_{ik,t})\underline{M} \le w_{i,t} - w_{k,t} \\ w_{i,t} - w_{k,t} \le 2(r_{ik}p_{ik,t} + x_{ik}q_{ik,t}) + (1-\ell_{ik,t})\overline{M} \end{aligned} \tag{2}$$

where $\underline{M}$ and $\overline{M}$ are big-M constants computed from voltage magnitude limits. This constraint ensures that if line (i,k) is energized, the voltage magnitude difference between buses i and k follows the LinDistFlow equations, but if line (i,k) is de-energized, the voltage magnitude difference is unconstrained. To see how to compute the big-M constants, note that if the line is energized, i.e., $\ell_{ik,t} = 1$, then the terms with big-M constants vanish from both inequalities and the voltage magnitude difference follows the LinDistFlow equations. However, if the line is de-energized and thus $\ell_{ik,t} = 0$, then we must allow $w_{k,t} - w_{i,t}$ to take on any possible values. Since voltage magnitudes at every bus are constrained by (5), we can easily compute $\underline{M} = \underline{V}_i^2 - \overline{V}_k^2$ and $\overline{M} = \overline{V}_i^2 - \underline{V}_k^2$. Note that by (1) we know that if $\ell_{ik,t} = 0$ then $p_{ik,t} = q_{ik,t} = 0$, so we need not consider the term $2(r_{ik}p_{ik,t} + x_{ik}q_{ik,t})$ when computing the big-M constants.

For all $t \in \mathcal{T}$, we apply power balance constraints:

$$\begin{aligned} p_{ik,t} = -P_{k,t} + \sum_{m:k\to m} p_{km,t} \quad \forall (i,k) \in \mathcal{L}^{\mathcal{H}} \\ q_{ik,t} = -Q_{k,t} + \sum_{m:k\to m} q_{km,t} \quad \forall (i,k) \in \mathcal{L}^{\mathcal{H}} \end{aligned} \tag{3}$$

Here, $P_{i,t}$ and $Q_{i,t}$ represent the active and reactive power injections, respectively, at bus i.

At each bus $i \in \mathcal{N}^{\mathcal{H}}$, the injected power is given by

$$\begin{aligned} P_{i,t} = \sum_{m\in\mathcal{G}_i} P^g_{m,t} - \sum_{m\in\mathcal{D}_i} P^d_{m,t} \\ Q_{i,t} = \sum_{m\in\mathcal{G}_i} Q^g_{m,t} - \sum_{k\in\mathcal{D}_i} Q^d_{m,t} \end{aligned} \tag{4}$$

where $P^g_{m,t}$ and $Q^g_{m,t}$ denote the active and reactive power generated at generator m at time t, and $P^d_{m,t}$ and $Q^d_{m,t}$ denote the active and reactive power consumed at load m at time t. Also, $\mathcal{D}_i$ denotes the set of loads at bus i and $\mathcal{G}_i$ denotes the set of generators at bus i.

We also bound the voltage magnitudes at all buses:

$$\underline{V}_i^2 \leq w_{i,t} \leq \overline{V}_i^2 \quad \forall i \in \mathcal{N}^{\mathcal{H}},\ \forall t \in \mathcal{T} \tag{5}$$

We may also want to ensure that the transmission network remains connected after switching. To do so, we use a network flow formulation that introduces an artificial commodity as in [15]. The reference bus supplies $\mathcal{N}^{\mathcal{H}} - 1$ units of the commodity, and every other bus must consume one unit. Let $\mathcal{S}$ denote the one-element set containing the reference bus. We introduce artificial flow variables $f_{ik,t}$ across each branch (i,k). The constraint for artificial commodity flow balance at each node other than the reference bus is

$$\sum_{k:i\to k} f_{ik,t} - \sum_{k:k\to i} f_{ik,t} = 1 \quad \forall i \in \mathcal{N}^{\mathcal{H}} \setminus \mathcal{S}, \quad \forall t \in \mathcal{T} \tag{6}$$

In addition, we ensure that no artificial commodity can flow across a de-energized line:

$$\begin{aligned} &\forall t \in \mathcal{T}: \\ &-(|\mathcal{N}^{\mathcal{H}}|-1)\ell_{ik,t} \leq f_{ik,t} \leq (|\mathcal{N}^{\mathcal{H}}|-1)\ell_{ik,t} \quad \forall (i,k) \in \mathcal{L}^{\mathcal{H}} \end{aligned} \tag{7}$$

By requiring each non-reference bus to consume one unit of this artificial commodity and restricting flows of the artificial commodity to the energized lines only, these constraints ensure that there exists some path across energized lines from the reference bus to every other bus in the network. Therefore, the network will remain connected after switching if these artificial flow constraints are imposed. Note that these artificial flows are a simple way of ensuring connectivity, but more sophisticated methods which minimize the number of constraints needed to maintain network connectedness during optimal transmission switching have been explored in, e.g., [16] and could be applied in our formulation.

B. Distribution Constraints

We model three-phase power flow in unbalanced distribution networks with battery storage and load shedding. For simplicity, we model ideal batteries with perfect efficiency, and we model a continuous load shed at every load. Note that we use a bold notation to indicate a vector of variables which contains values for all phases of the bus or line. For example, for a three-phase bus,

$$\boldsymbol{w}_{i,t} = \begin{bmatrix} w_{i,t}^a & w_{i,t}^b & w_{i,t}^c \end{bmatrix}^T$$

Using the same notation as in Section II-A, we denote the squared voltage magnitudes at bus i at time t as $\boldsymbol{w}_{i,t}$. The active and reactive power flows across line (i,k) are $\boldsymbol{p}_{ik,t}$ and $\boldsymbol{q}_{ik,t}$. The resistance is $\boldsymbol{r}_{ik}$ and the reactance is $\boldsymbol{x}_{ik}$. When modeling all phases in the distribution network, $\boldsymbol{r}_{ik}$ and $\boldsymbol{x}_{ik}$ are matrices with terms that reflect self-impedance as well as mutual impedances between phases. For all $(i,k) \in \mathcal{L}^{\mathcal{D}}$ and $t \in \mathcal{T}$, the difference in squared voltage magnitudes between buses i and k is

$$\boldsymbol{w}_{k,t} = \boldsymbol{w}_{i,t} - \boldsymbol{M}_{ik,t}^P \boldsymbol{p}_{ik,t} - \boldsymbol{M}^Q \boldsymbol{q}_{ik,t} \tag{8}$$

where we have that

$$\boldsymbol{\Gamma} = \begin{bmatrix} 1 & \alpha^2 & \alpha \\ \alpha & 1 & \alpha^2 \\ \alpha^2 & \alpha & 1 \end{bmatrix}$$

for $\alpha = \exp(-j\frac{2\pi}{3})$ and

$$\begin{aligned} \boldsymbol{M}^P &= 2\big(\Re(\boldsymbol{\Gamma}) \odot \boldsymbol{r}_{ik} + \Im(\boldsymbol{\Gamma}) \odot \boldsymbol{x}_{ik}\big) \\ \boldsymbol{M}^Q &= 2\big(\Re(\boldsymbol{\Gamma}) \odot \boldsymbol{x}_{ik} - \Im(\boldsymbol{\Gamma}) \odot \boldsymbol{r}_{ik}\big) \end{aligned}$$

where we denote $\boldsymbol{A} \odot \boldsymbol{B}$ as the element-wise product of $\boldsymbol{A}$ and $\boldsymbol{B}$. Also note that $j = \sqrt{-1}$, and $\Re$ and $\Im$ are the real and imaginary part operators, respectively.

For all $t \in \mathcal{T}$, power balance is given by

$$\begin{aligned} \boldsymbol{p}_{ik,t} &= -\boldsymbol{P}_{k,t} + \sum_{m:k\to m} \boldsymbol{p}_{km,t} \quad \forall (i,k) \in \mathcal{L}^{\mathcal{D}} \\ \boldsymbol{q}_{ik,t} &= -\boldsymbol{Q}_{k,t} + \sum_{m:k\to m} \boldsymbol{q}_{km,t} \quad \forall (i,k) \in \mathcal{L}^{\mathcal{D}} \end{aligned} \tag{9}$$

where $\boldsymbol{P}_{k,t}$ and $\boldsymbol{Q}_{k,t}$ represent active and reactive power injections at bus k.

The formulation also allows load shedding, which may be necessary given transmission line de-energizations. Previous papers on transmission line switching generally model a continuous load shed at bulk transmission loads [2], [3]. We model a continuous load shedding at individual distribution loads. In practice, load shedding would be actuated by opening switches in the distribution networks. Our future work includes more accurately modeling load shedding by making binary switching decisions to de-energize blocks of loads in the distribution network. For the purposes of this paper, we use a continuous variable $s_{i,t} \in [0,1]$ to denote the proportion of load served at bus i at time t. For example, if $s_{i,t} = 0.8$, then 20% of the load at bus i is shed during time period t. The power injections at each bus account for storage devices and load shedding at that bus:

$$\begin{aligned} \boldsymbol{P}_{i,t} &= \sum_{m\in\mathcal{S}_i} \boldsymbol{P}_{m,t}^s - s_{i,t} \sum_{m\in\mathcal{D}_i} \boldsymbol{P}_{m,t}^d \\ \boldsymbol{Q}_{i,t} &= \sum_{m\in\mathcal{S}_i} \boldsymbol{Q}_{m,t}^s - s_{i,t} \sum_{m\in\mathcal{D}_i} \boldsymbol{Q}_{m,t}^d \end{aligned} \tag{10}$$

Here, $\boldsymbol{P}_{m,t}^s$ and $\boldsymbol{Q}_{m,t}^s$ represent active and reactive power injections from storage device m at time t. Similarly, $\boldsymbol{P}_{m,t}^d$ and $\boldsymbol{Q}_{m,t}^d$ represent the active and reactive power demands from load m at time t.

We also limit the voltage magnitudes at bus i as

$$\underline{\boldsymbol{V}}_i^2 \leq \boldsymbol{w}_{i,t} \leq \overline{\boldsymbol{V}}_i^2 \quad \forall i \in \mathcal{N}^{\mathcal{D}}, \quad \forall t \in \mathcal{T} \tag{11}$$

where $\underline{\boldsymbol{V}}_i^2$, $\overline{\boldsymbol{V}}_i^2$ are vectors of the lower and upper bounds, respectively, on the squared voltage magnitudes at bus i.

Each distribution network may contain battery energy storage systems. We use an ideal storage model with perfectly efficient charging and discharging. The variable C_i is positive when the storage system is charging and negative when it is discharging. The state of charge E_i is bounded by its

energy capacity $\overline{E}_i$. There are also bounds on the charging/discharging power, where $\underline{C}_i$ denotes the lower bound that limits discharging power and $\overline{C}_i$ is the upper bound which limits its charging power. We assume that the charging/discharging power C_i is fixed during each time period $t \in \mathcal{T}$:

$$\boldsymbol{E}_{i,t} - \boldsymbol{E}_{i,t-1} = \boldsymbol{C}_i \qquad \forall i \in \mathcal{N}^{\mathcal{D}} \tag{12}$$

$$0 \leq \boldsymbol{E}_{i,t} \leq \overline{\boldsymbol{E}_i} \qquad \forall i \in \mathcal{N}^{\mathcal{D}} \tag{13}$$

$$\underline{\boldsymbol{C}}_i \leq \boldsymbol{C}_i \leq \overline{\boldsymbol{C}}_i \qquad \forall i \in \mathcal{N}^{\mathcal{D}} \tag{14}$$

C. Transmission-Distribution Boundary

We collect the buses at transmission-distribution boundaries into a set β containing tuples $(b^{\mathcal{H}}, b^{\mathcal{D}}) \in \beta$ where $b^{\mathcal{H}}$ is the transmission bus and $b^{\mathcal{D}}$ is the distribution bus. On the transmission side, we have modeled single-phase equivalent power flow from each transmission boundary bus $b^{\mathcal{H}}$ to the corresponding distribution boundary bus $b^{\mathcal{D}}$. On the distribution side, we have modeled three-phase power flow from the distribution boundary bus to its corresponding transmission bus. To ensure that these power flows are consistent, we impose the following constraints:

$$\begin{aligned} &\forall (b^{\mathcal{H}}, b^{\mathcal{D}}) \in \beta,\ \forall t \in \mathcal{T}: \\ &p^{\mathcal{H}}_{b^{\mathcal{H}} b^{\mathcal{D}},t} + \sum_{\phi \in \Phi_{b^{\mathcal{D}}}} p^{\mathcal{D},\phi}_{b^{\mathcal{D}} b^{\mathcal{H}},t} = 0 \\ &q^{\mathcal{H}}_{b^{\mathcal{H}} b^{\mathcal{D}},t} + \sum_{\phi \in \Phi_{b^{\mathcal{D}}}} q^{\mathcal{D},\phi}_{b^{\mathcal{D}} b^{\mathcal{H}},t} = 0 \end{aligned} \tag{15}$$

where Φ_i is the set of phases at a given bus i. The constraints in (15) ensure that the transmission model's power flow across the boundary toward the distribution side is equal and opposite to the sum across all phases in Φ_i of the distribution model's power flow across the boundary toward the transmission side. We also require that voltage magnitudes on either side of the boundary bus are equal:

$$w^{\mathcal{H}}_{b^{\mathcal{H}},t} = w^{\mathcal{D},\phi}_{b^{\mathcal{D}},t}, \quad \forall \phi \in \Phi_{b^{\mathcal{D}}},\ \forall (b^{\mathcal{H}}, b^{\mathcal{D}}) \in \beta,\ \forall t \in \mathcal{T} \tag{16}$$

This formulation results in balanced voltage magnitudes at distribution substations, an assumption made by the integrated transmission-distribution software in our experiments [14].

D. Objective Function

To these constraints, we add an objective function inspired by [2], [3], which balances wildfire risk with load shedding:

$$\begin{aligned} C(\boldsymbol{\ell}, \boldsymbol{s}) = \sum_{t \in \mathcal{T}} \Big[&\gamma \sum_{(i,k) \in \mathcal{L}^{\mathcal{H}}} \rho_{ik,t} \ell_{ik,t} \\ &+ (1-\gamma) \big(\sum_{i \in \mathcal{N}^{\mathcal{D}}} s_{i,t} \sum_{\phi \in \Phi_i} -P^{d,\phi}_{i,t} \big) \Big] \end{aligned} \tag{17}$$

Here, ρ_{ik} is the wildfire ignition risk for line (i,k) at time t, and $P^{d,\phi}_{i,t}$ is the active power demand at phase ϕ of bus i during time period t. Also, the parameter γ allows controlling the tradeoff between load shedding and wildfire risk. The cost function depends on both $\boldsymbol{\ell}$, the vector of all transmission line energization statuses, and $\boldsymbol{s}$, the vector of all bus load sheds.

To summarize, the optimal switching problem for wildfire risk mitigation is the following mixed-integer linear program:

$$\begin{aligned} \min_{\substack{\boldsymbol{\ell}^{\mathcal{H}}, \boldsymbol{p}^{\mathcal{H}}, \boldsymbol{q}^{\mathcal{H}}, \boldsymbol{w}^{\mathcal{H}}, \\ \boldsymbol{s}^{\mathcal{D}}, \boldsymbol{p}^{\mathcal{D}}, \boldsymbol{q}^{\mathcal{D}}, \boldsymbol{w}^{\mathcal{D}}, \boldsymbol{C}^{\mathcal{D}}, \boldsymbol{E}^{\mathcal{D}}}} \quad & (17) \\ \text{s.t.} \quad & (1) - (16) \end{aligned} \tag{18}$$

III. Decomposition and Distributed Optimization

We solve the large-scale optimal switching problem by decomposing other space and time with ADMM. Figure 1 shows how a small example system is decomposed, where each block represents a separate subproblem. The dashed lines represent coupling constraints between the central transmission network and its attached distribution networks at each time period. At the transmission level, we decompose across time periods to manage complexity from binary switching variables. Distribution subproblems cover all time periods because energy storage introduces many state-of-charge constraints that couple time periods. Decomposing distribution networks over time would result in thousands of coupling constraints between subproblems, slowing convergence.

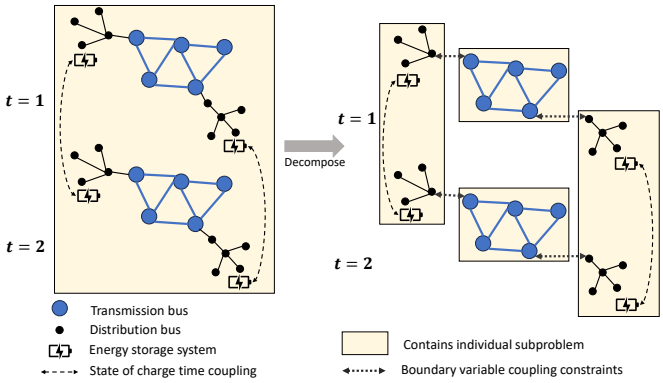

Fig. 1: This figure shows the decomposition of the multi-period problem. Dashed lines show the time coupling between energy storage systems' states of charge. After decomposition, each transmission network at each time period forms a subproblem. Each distribution network across all time periods forms a subproblem. Dotted lines show the coupling constraints between subproblems' copies of boundary variables.

Since transmission subproblems cover one time period, there are $|\mathcal{T}|$ transmission subproblems, which take the form

$$\begin{aligned} \min_{\substack{\boldsymbol{\ell}^{\mathcal{H}}, \boldsymbol{p}^{\mathcal{H}}, \boldsymbol{q}^{\mathcal{H}}, \boldsymbol{w}^{\mathcal{H}} \\ \boldsymbol{p}^{\mathcal{D}}, \boldsymbol{q}^{\mathcal{D}}}} \quad & \gamma \sum_{t \in \mathcal{T}} \sum_{(i,k) \in \mathcal{L}^{\mathcal{H}}} \rho_{ik,t} \ell_{ik,t} \\ \text{s.t.} \quad & (1) - (7) \end{aligned} \tag{19}$$

The number of distribution subproblems is equal to the number of distinct distribution networks. These distribution subproblems take the form

$$\begin{aligned} \min_{\substack{\boldsymbol{p}^{\mathcal{H}}, \boldsymbol{q}^{\mathcal{H}}, \boldsymbol{s}^{\mathcal{D}}, \\ \boldsymbol{p}^{\mathcal{D}}, \boldsymbol{q}^{\mathcal{D}}, \boldsymbol{w}^{\mathcal{D}}, \boldsymbol{C}^{\mathcal{D}}, \boldsymbol{E}^{\mathcal{D}}}} \quad & (1-\gamma) \sum_{t \in \mathcal{T}} \big(\sum_{i \in \mathcal{N}^{\mathcal{D}}} s_i \sum_{\phi \in \Phi_i} -P^{d,\phi}_{i,t} \big) \\ \text{s.t.} \quad & (8) - (14) \end{aligned} \tag{20}$$

To model the interaction between transmission and distribution subproblems, we introduce virtual buses at their boundaries. For transmission subproblems, the distribution network is represented by a three-phase virtual bus with a generator that can inject or consume unlimited active and reactive power. Similarly, each distribution subproblem includes a copy of the transmission boundary bus with a virtual generator.

The ADMM algorithm [17] solves the general problem

$$\begin{aligned} \min_{\boldsymbol{x}\in\mathcal{X},\boldsymbol{z}\in\mathcal{Z}} \quad & f(\boldsymbol{x}) + g(\boldsymbol{z}) \\ \text{s.t.} \quad & A\boldsymbol{x} + B\boldsymbol{z} = \boldsymbol{c} \end{aligned} \tag{21}$$

To write the decomposed optimal power shut-off problem in ADMM form (21), we collect the variables belonging to every subproblem in a vector $\boldsymbol{x}$. That is, $\boldsymbol{x}$ contains variables from transmission subproblems representing the lines' power flows $\boldsymbol{p}^{\mathcal{H}}, \boldsymbol{q}^{\mathcal{H}}$, the lines' energization statuses $\boldsymbol{\ell}$, the buses' squared voltages $\boldsymbol{w}^{\mathcal{H}}$, the buses' power injections $\boldsymbol{P}^{\mathcal{H}}, \boldsymbol{Q}^{\mathcal{H}}$, and artificial flows for connectivity $\boldsymbol{f}$. From the distribution subproblems, $\boldsymbol{x}$ also contains variables representing the lines' power flows $\boldsymbol{p}^{\mathcal{D}}, \boldsymbol{q}^{\mathcal{D}}$, the buses' squared voltages $\boldsymbol{w}^{\mathcal{D}}$, the buses' power injections $\boldsymbol{P}^{\mathcal{D}}, \boldsymbol{Q}^{\mathcal{D}}$, the buses' load sheds $\boldsymbol{s}^{\mathcal{D}}$, the battery energy storage systems' states of charge $\boldsymbol{E}^{\mathcal{D}}$, and the batteries' charging/discharging power $\boldsymbol{C}^{\mathcal{D}}$. Here we have indexed variables with $\mathcal{H}$ and $\mathcal{D}$ to indicate whether they belong to the transmission or distribution systems, respectively. We must also include in $\boldsymbol{x}$ the voltage magnitude and power injection variables at *virtual* buses in the subproblems.

Next, we introduce a "central" copy of the variables at the virtual buses, and gather these central variables into a vector $\boldsymbol{z}$. This formulation with "central" variables allows us to use the ADMM algorithm, which is designed to optimize over two sets of variables with simple coupling constraints, to solve a problem with parallel subproblems over many regions of the power system. Let the tilde notation indicate central variables in the vector $\boldsymbol{z}$, so that, for example, $\tilde{w}_m$ is the central copy of the squared voltage magnitude at bus m. For a transmission subproblem with boundary bus m and virtual distribution boundary bus n', the constraints are as follows:

$$\begin{aligned} & w_m = \tilde{w}_m \\ & w_{n'_\phi} = \tilde{w}_{n_\phi} \quad \forall \phi \in \Phi_n \end{aligned} \tag{22}$$

$$\begin{aligned} & p_{mn'} = \tilde{p}_{mn}, \quad q_{mn'} = \tilde{q}_{mn} \\ & p_{n'_\phi m_\phi} = \tilde{p}_{n_\phi m_\phi}, \quad q_{n'_\phi m_\phi} = \tilde{q}_{n_\phi m_\phi} \quad \forall \phi \in \Phi_n \end{aligned} \tag{23}$$

Similarly, for a distribution subproblem with boundary bus n and virtual transmission boundary bus m', the constraints are:

$$\begin{aligned} & w_{m'} = \tilde{w}_m \\ & w_{n_\phi} = \tilde{w}_{n_\phi} \quad \forall \phi \in \Phi_n \end{aligned} \tag{24}$$

$$\begin{aligned} & p_{m'n} = \tilde{p}_{mn}, \quad q_{m'n} = \tilde{q}_{mn} \\ & p_{n_\phi m'_\phi} = \tilde{p}_{n_\phi m_\phi}, \quad q_{n_\phi m'_\phi} = \tilde{q}_{n_\phi m_\phi} \quad \forall \phi \in \Phi_n \end{aligned} \tag{25}$$

The constraints (22) and (24) ensure that the transmission and distribution subproblems agree on voltage magnitudes at the boundary, while the constraints (23) and (25) ensure that the transmission and distribution subproblems agree on power flows across the boundary.

The ADMM algorithm augments the Lagrangian function for (21) with a penalty term. The augmented term typically penalizes the squared ℓ_2-norm of the coupling constraint violations, $||A\boldsymbol{x}+B\boldsymbol{z}-\boldsymbol{c}||_2^2$. However, quadratic programs may experience more numerical problems compared to linear programs during execution of Gurobi's simplex or interior-point algorithms [18]. To improve subproblem numerics, we run the ADMM algorithm on the ℓ_1-norm augmented Lagrangian:

$$\begin{aligned} L_\alpha(\boldsymbol{x}, \boldsymbol{z}, \boldsymbol{\lambda}) = f(\boldsymbol{x}) + g(\boldsymbol{z}) + \boldsymbol{\lambda}^T(A\boldsymbol{x} + B\boldsymbol{z} - \boldsymbol{c}) \\ + \alpha||A\boldsymbol{x} + B\boldsymbol{z} - \boldsymbol{c}||_1 \end{aligned} \tag{26}$$

Here, $\boldsymbol{\lambda}$ contains the dual variables for each coupling constraint in (21). The penalty parameter α is user-selected.

At each iteration k, the ADMM algorithm minimizes over the $\boldsymbol{x}$ and $\boldsymbol{z}$ variables separately, while holding all other variables fixed, and then updates the dual variables. The variable updates at iteration k are as follows:

$$\boldsymbol{x}^{k+1} = \arg\min_{\boldsymbol{x}} L_\alpha(\boldsymbol{x}, \boldsymbol{z}^k, \boldsymbol{\lambda}^k) \tag{27}$$

$$\boldsymbol{z}^{k+1} = \arg\min_{\boldsymbol{z}} L_\alpha(\boldsymbol{x}^{k+1}, \boldsymbol{z}, \boldsymbol{\lambda}^k) \tag{28}$$

$$\boldsymbol{\lambda}^{k+1} = \boldsymbol{\lambda}^k + \alpha(A\boldsymbol{x} + B\boldsymbol{z} - \boldsymbol{c}) \tag{29}$$

The $\boldsymbol{x}$-update step corresponds to solving all transmission and distribution subproblems in parallel. The transmission and distribution subproblems are in (19) and (20), respectively, but the relaxed coupling constraints augmented with the ℓ_1-norm penalty as shown in (26) are added to the objective. The transmission subproblems are mixed-integer linear programs, while the distribution subproblems are linear programs. Transmission subproblems cover single time periods and scale according to the number of buses and branches in the system. Distribution subproblems cover all time periods and scale according to the number of buses, lines, switches, and storage systems in the system.

IV. Case Study

We construct a test case using the CATS (California Test System) [19] and SMART-DS synthetic distribution networks [20]. We attach eight distribution networks from the SMART-DS San Francisco dataset to a section of the CATS system in the San Francisco region. We place battery energy storage systems randomly at 30% of the low-voltage nodes in the distribution networks, each with energy capacity randomly selected between 45 and 100 kilowatt-hours. Next, we aggregate distribution loads and the energy capacities of storage devices at voltage levels below 7 kV. The full test case contains buses and lines at voltage levels from 7 kV through 230 kV. The transmission system consists of 155 buses, 15 generators, and 171 branches. The distribution system, across all networks, contains 15,083 buses, 15,496 lines and 1203 battery energy storage systems. Since optimizing over the unbalanced distribution system requires modeling each phase separately, we also note that there are 24,823 individual nodes

across all buses. Wildfire ignition risk values are selected using the "high-risk cumulative" metric described in [21], based on the wind-enhanced fire potential index (WFPI) from the United States Geological Survey [22].

All experiments ran on the Georgia Institute of Technology PACE high-performance computing cluster. Each experiment consisted of solving the optimal switching problem for wildfire risk mitigation over some number of time periods $\mathcal{T}$, using one PACE CPU compute node equipped with two 12-core 2.7 GHz processors and 192 GB RAM. Any algorithm that did not converge within a 48-hour time period was terminated. We first present results with the connectivity constraints (6)–(7) included. We compare distributed and centralized computation times, evaluate the effect of coordinated transmission-distribution switching, and discuss whether the distributed method finds optimal solutions. Next, we present results for the optimal switching problem without the connectivity constraints. For our problem, this significantly reduces wildfire risk but increases computation time.

A. Comparing Central and Distributed Computation Time

We compare a centralized solution method, which solves the full MILP directly with Gurobi, to the distributed solution method described in Section III. We terminate the central solution method when the MIP gap reaches 0.1%, and also solve distributed subproblems to a 0.1% MIP gap. We terminate the distributed algorithm when the norm of the mismatches between subproblems' shared variables falls below $\epsilon = 10^{-4}$.

Figure 2 shows the runtimes for each method as we increase the number of periods in the multi-period problem. When the problem is sufficiently large, we see that the distributed method performs much better than the centralized method (e.g., approximately an order-of-magnitude faster with eight periods). In the future, we could potentially achieve further computational speedups by distributing suproblems across multiple computing nodes in addition to the parallelization across computing cores as in this paper.

For nine or more time periods, the central method fails to converge within 48 hours, at which point the MIP gap is 54.1% or higher. The distributed method also fails to find the optimal solution for nine or more time periods, converging to a sub-optimal solution which may be more costly than simply solving a transmission switching problem without accounting for distribution network flexibility. We discuss the problem of sub-optimality further below in Section IV-C.

B. Effect of Coordinated Transmission-Distribution Switching

We show how solving an ITD optimal switching problem produces transmission switching decisions that reduce wildfire ignition risk more than solving only a transmission-level problem. The "transmission-only" problem neglects energy storage in distribution networks and places aggregate loads at the distribution boundary buses. We present results for the optimal switching problem solved over eight time periods, the highest number of periods for which the distributed algorithm reached the optimal solution. Figure 3a shows the total wildfire

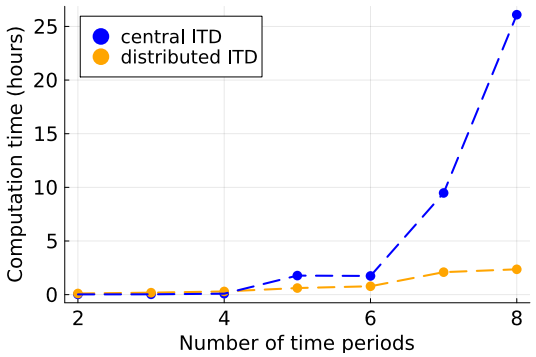

Fig. 2: Comparing computation time for the central solution method using the Gurobi solver vs. our distributed solution method.

risk, i.e., the sum of the risk values on all energized lines, at each period. Observe that the ITD problem selects different switching decisions than the transmission-only problem, which slightly reduces the wildfire ignition risk for the last two time periods. Although risk reduction was relatively small for this test case, it could be more significant for scenarios with more high-risk transmission lines. Figure 3b shows the total load shed in MW at each time period t. The ITD problem leverages distribution energy storage systems to schedule less load shedding compared to the transmission-only problem.

C. Discussion on Optimality

Although ADMM does not provide convergence guarantees for non-convex problems, previous work suggests that ADMM can find good solutions to mixed-integer problems [10]–[12]. For our problem, the centralized solver converged within 48 hours for the 2-, 3-, 4-, 5-, 6-, 7- and 8-period cases, enabling a comparison between the centralized and distributed solutions. Our metric is the cost percent difference between the central objective cost f^c and the distributed objective cost f^d, computed as $(f^d - f^c)/f^c$. The cost percent difference is less than 0.1% (the MIP gap tolerance) for all these cases.

However, over nine or more time periods, the distributed approach converged to a sub-optimal solution. Lacking a centralized solution for nine or more time periods, we used the "transmission-only" solution described in Section IV-B for comparison. The transmission-only problem models each distribution network as an aggregate load, neglecting the energy storage systems. Clearly, the optimal ITD solution, which leverages energy storage to support loads, should be no more costly than the optimal transmission-only solution. For cases with nine or more periods, the distributed algorithm converged to a sub-optimal solution with higher cost than the "transmission-only" solution.

Our future work will investigate improvements to the distributed algorithm to achieve better solutions for large multi-period problems. The authors of [12] suggest using ADMM as a heuristic, running the distributed algorithm several times with different penalty parameters and initializations and selecting the best result. We may also explore better methods for

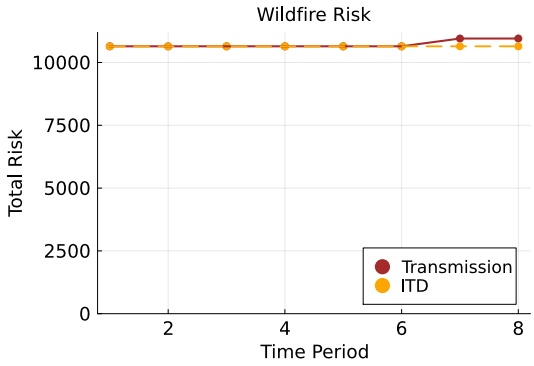

(a) Comparing the total wildfire risk, i.e., the sum of risk values on all energized lines, between the transmission-only problem and the ITD problem.

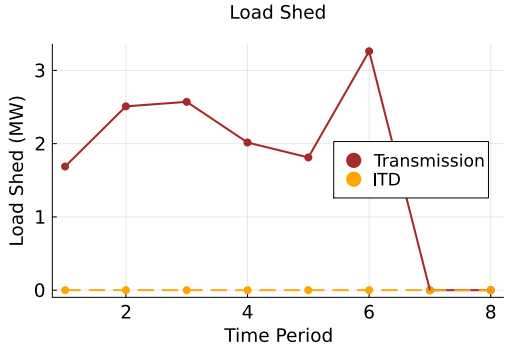

(b) Comparing the total load shed in MW between the transmission-only problem and the ITD problem.

Fig. 3: This figure compares results from the ITD optimal switching problem to a transmission-only switching problem that neglects the distribution network storage systems. The ITD problem makes switching decisions which reduce wildfire risk compared to the transmission-only problem, and schedules less load shedding.

initializing the primal and dual variables associated with the coupling constraints, perhaps by solving some transmission-level problem with reduced models of the distribution networks. We may also leverage new machine learning techniques to perform data-driven penalty parameter tuning, such as the reinforcement learning approach in [23].

D. Removing Connectivity Constraints

In this section, we explore solving the optimal switching problem without connectivity constraints (6)–(7) that require the transmission network to remain fully connected after switching. In Figure 4, we compare the computation time for the centralized solver, Gurobi, with the computation time for our distributed method. Without the connectivity constraints, the optimal switching problem takes longer to solve, and for six or more time periods the centralized solver fails to converge within 48 hours. The distributed algorithm fails to converge within 48 hours for seven or more time periods. We also perform the comparison described in Section IV-B to demonstrate the effect of solving an ITD problem rather than a transmission-only problem. The effect is more significant here than in Section IV-B because removing the connectivity constraints increases the number of transmission lines which may be de-energized. Figure 5a shows the total wildfire risk, or the sum of risk values on all energized lines, and Figure 5b shows the total load shed in MW. The ITD problem de-energizes enough risky transmission lines that the total wildfire risk is near zero across all time periods.

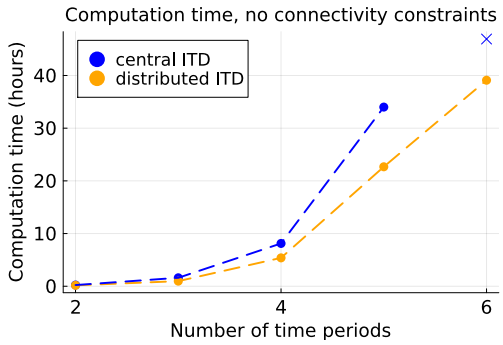

Fig. 4: Comparing computation time for the optimal switching problem without connectivity constraints for the central solution method using the Gurobi solver vs. our distributed solution method.

For this test case, when the transmission network is not required to be fully connected, solving the ITD optimal switching problem significantly reduces wildfire risk and schedules less load shedding compared to the transmission-only problem. Although the distributed algorithm converges more quickly than the centralized solver, it is still too slow to find a good solution for more than seven time periods.

V. Conclusion

This paper presents a coordinated transmission-distribution optimal switching problem to reduce wildfire ignition risk while minimizing load shedding. To address the computational challenges of solving the multi-period mixed-integer linear program on a large-scale test case, we explore a distributed solution method. We propose decomposing the problem over space and time into smaller subproblems. Then, we use an ADMM-based distributed algorithm to solve the decomposed problem. Given the same computing resources, our distributed method significantly outperforms the centralized solver on some problems. We also find that the coordinated transmission-distribution problem, which leverages battery energy storage systems in the distribution networks to support loads, selects different line de-energizations which reduce wildfire risk compared to solving only a transmission-level problem.

However, the distributed algorithm does not provide optimality guarantees for mixed-integer programs, and reached sub-optimal solutions for sufficiently large problems. When attempting to solve the optimal switching problem over more than eight time periods, the centralized solver failed to converge and the distributed algorithm converged to a sub-optimal solution. Our future work includes improving the distributed

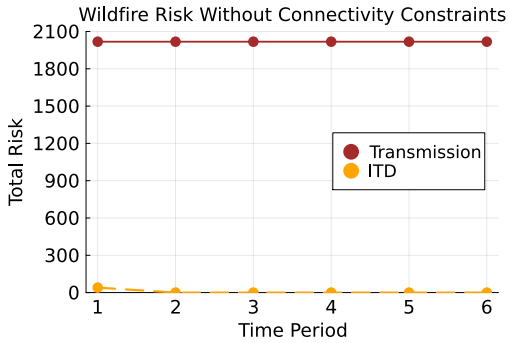

(a) Comparing the total wildfire risk, i.e., the sum of risk values on all energized lines, between the transmission-only problem and the ITD problem when solving without connectivity constraints.

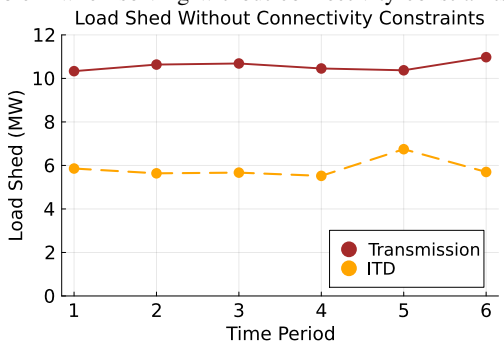

(b) Comparing the total load shed in MW between the transmission-only problem and the ITD problem when solving without connectivity constraints.

Fig. 5: This figure performs the same comparison as Figure 3 between the wildfire risk and load shedding computed by the ITD optimal switching problem and the transmission-only optimal switching problem. However, this figure presents results for solving the problem without requiring the transmission network to remain fully connected. In this case, the ITD problem significantly reduces wildfire risk by de-energizing more transmission lines than the transmission-only problem, and using distribution network storage systems to support loads.

algorithm's convergence performance. Potential directions include finding better initializations and using machine learning for data-driven penalty parameter tuning. We also intend to make the load shed model more realistic by making switching decisions at the distribution level to de-energize blocks of loads.

References

[1] Pacific Gas and Electric Company (PG&E), "2023-2025 Wildfire Mitigation Plan," 2024. [Online]. Available: https://www.pge.com/assets/pge/docs/outages-and-safety/outage-preparedness-and-support/2024-06-07-PGE-2023-WMP-R4-1.pdf

[2] N. Rhodes, L. Ntaimo, and L. Roald, "Balancing Wildfire Risk and Power Outages Through Optimized Power Shut-Offs," *IEEE Trans. Power Syst.*, vol. 36, no. 4, pp. 3118–3128, 2021.

[3] A. Kody, A. West, and D. K. Molzahn, "Sharing the Load: Considering Fairness in De-energization Scheduling to Mitigate Wildfire Ignition Risk using Rolling Optimization," in *61st IEEE Conference on Decision and Control (CDC)*, 2022, pp. 5705–5712.

[4] S. Taylor, G. Setyawan, B. Cui, A. Zamzam, and L. A. Roald, "Managing Wildfire Risk and Promoting Equity through Optimal Configuration of Networked Microgrids," in *ACM e-Energy*, 2023, p. 189–199.

[5] Y. Zhou, A. Zamzam, and A. Bernstein, "Equitable Networked Microgrid Topology Reconfiguration for Wildfire Risk Mitigation," Feb. 2024, arXiv:2402.04444.

[6] J. Su, S. Mehrani, P. Dehghanian, and M. A. Lejeune, "Quasi Second-Order Stochastic Dominance Model for Balancing Wildfire Risks and Power Outages due to Proactive Public Safety De-Energizations," *IEEE Trans. Power Syst.*, vol. 39, no. 2, pp. 2528–2542, 2024.

[7] Q. Wang, W. Wu, C. Lin, Y. Yang, and B. Wang, "A Spatio-Temporal Decomposition Method for the Coordinated Economic Dispatch of Integrated Transmission and Distribution Grids," *IEEE Trans. Power Syst.*, vol. 39, no. 3, pp. 4835–4851, 2024.

[8] M. K. Arpanahi, M. E. H. Golshan, and P. Siano, "A Comprehensive and Efficient Decentralized Framework for Coordinated Multiperiod Economic Dispatch of Transmission and Distribution Systems," *IEEE Systems Journal*, vol. 15, no. 2, pp. 2583–2594, 2021.

[9] Z. Chen, Z. Li, C. Guo, J. Wang, and Y. Ding, "Fully Distributed Robust Reserve Scheduling for Coupled Transmission and Distribution Systems," *IEEE Trans. Power Syst.*, vol. 36, no. 1, pp. 169–182, 2021.

[10] R. Takapoui, N. Moehle, S. Boyd, and A. Bemporad, "A Simple Effective Heuristic for Embedded Mixed-Integer Quadratic Programming," in *American Control Conference (ACC)*, 2016, pp. 5619–5625.

[11] A. Alavian and M. C. Rotkowitz, "Improving ADMM-based optimization of Mixed Integer Objectives," in *51st Annual Conference on Information Sciences and Systems (CISS)*, 2017.

[12] Y. Kanno and S. Kitayama, "Alternating Direction Method of Multipliers as a Simple Effective Heuristic for Mixed-Integer Nonlinear Optimization," *Structural and Multidisciplinary Optimization*, vol. 58, no. 3, p. 1291–1295, September 2018.

[13] L. Gan and S. H. Low, "Convex Relaxations and Linear Approximation for Optimal Power Flow in Multiphase Radial Networks," in *18th Power Systems Computation Conference (PSCC)*, 2014.

[14] J. Ospina, D. M. Fobes, R. Bent, and A. Wächter, "Modeling and Rapid Prototyping of Integrated Transmission-Distribution OPF Formulations With PowerModelsITD.jl," *IEEE Trans. Power Syst.*, vol. 39, no. 1, pp. 172–185, 2024.

[15] M. Numan, M. F. Abbas, M. Yousif, S. S. M. Ghoneim, A. Mohammad, and A. Noorwali, "The Role of Optimal Transmission Switching in Enhancing Grid Flexibility: A Review," *IEEE Access*, vol. 11, pp. 32 437–32 463, 2023.

[16] T. Han, Y. Song, and D. J. Hill, "Ensuring Network Connectedness in Optimal Transmission Switching Problems," *IEEE Trans. Circuits and Syst. II: Express Briefs*, vol. 68, no. 7, pp. 2603–2607, 2021.

[17] S. Boyd, N. Parikh, E. Chu, B. Peleato, and J. Eckstein, "Distributed Optimization and Statistical Learning via the Alternating Direction Method of Multipliers," *Foundations and Trends in Machine Learning*, vol. 3, no. 1, pp. 1–122, 2011.

[18] R. Luce, "Quadratic Optimization," Gurobi Optimization, Tech. Rep., 2022. [Online]. Available: https://cdn.gurobi.com/wp-content/uploads/quadratic_optimization.pdf

[19] S. Taylor, A. Rangarajan, N. Rhodes, J. Snodgrass, B. C. Lesieutre, and L. A. Roald, "California Test System (CATS): A Geographically Accurate Test System Based on the California Grid," *IEEE Trans. Energy Markets, Policy and Regulation*, vol. 2, no. 1, pp. 107–118, 2024.

[20] V. K. Krishnan *et al.*, "SMART-DS: Synthetic Models for Advanced, Realistic Testing: Distribution Systems and Scenarios," National Renewable Energy Laboratory (NREL), Tech. Rep., 2017.

[21] R. Piansky, S. Taylor, N. Rhodes, D. K. Molzahn, L. A. Roald, and J.-P. Watson, "Quantifying Metrics for Wildfire Ignition Risk from Geographic Data in Power Shutoff Decision-Making," in *58th Hawaii International Conference on System Sciences (HICSS)*, January 2025.

[22] United States Geological Survey (USGS), "Wildland Fire Potential Index," 2024. [Online]. Available: https://www.usgs.gov/fire-danger-forecast/wildland-fire-potential-index-wfpi

[23] S. Zeng, A. Kody, Y. Kim, K. Kim, and D. K. Molzahn, "A Reinforcement Learning Approach to Parameter Selection for Distributed Optimization in Power Systems," *Electric Power Systems Research*, vol. 212, p. 108546, 2022, presented at the *22nd Power Systems Computation Conference (PSCC 2022)*.